Chloride-Induced Corrosion of Cracked Cement-Based Composites

Gideon P.A.G. van Zijl[(✉)], Schalk R. Bezuidenhout,
and Algurnon S. van Rooyen

Division for Structural Engineering and Civil Engineering Informatics,
Stellenbosch University, Stellenbosch, South Africa
gvanzijl@sun.ac.za

Abstract. Chloride-induced corrosion tests in cracked steel reinforced SHCC (R/SHCC) beams have recently been reported by the research group in Stellenbosch, South Africa. The influence of crack spacing has been investigated, including Coulostatic corrosion rate measurements and actual observation and recorded corrosion damage in the steel bars in terms of mass loss and pitting depths. To further investigate the influence of crack spacing on chloride-induced corrosion in cement-based composites, comparative tests are currently performed on cracked reinforced concrete (R/C), as well as lightweight foam concrete (R/LWFC) beams. Locally developed Coulostatic equipment, and a polarisation technique with Gecor 10 equipment are used for non-destructive measurement of corrosion rate. R/SHCC, R/C and R/LWFC beams are subjected to imposed strain in special load frames, combined with cyclic chloride ponding on the cracked face to induce corrosion in the reinforcing bars. The observed corrosion rates in the respective cement-based beams are compared, and the influence of cover depth, rebar reinforcement level and crack spacing is investigated and reported. The comparative study has the objective to identify mechanisms of chloride-induced corrosion in the respective cement-based materials, towards understanding of this deterioration mechanism, and towards development of rational prediction models for durability design.

Keywords: SHCC · LWFC · RC · Corrosion · Chloride

1 Introduction

Chloride-induced corrosion is a major cause of deterioration in reinforced concrete infrastructure, in coastal environments and in regions where salt-based de-icing of roadways is common practice. Significant knowledge has been developed on the mechanisms, diagnosis and repair strategies of reinforced concrete. Recently developed cement-based material classes of strain-hardening cement-based composites (SHCC) and lightweight foam concrete (LWFC) require investigation into possibly changed mechanisms, and characterization towards prediction of corrosion, as well as possible prevention, maintenance and repair strategies.

The role of crack width in the ingress of chlorides into cracked cement-based composites (Djerbi et al. 2008) and SHCC in particular (Boshoff et al. 2016) has been

studied and reported, indicating a threshold crack width of about 0.03 mm to allow chloride ingress, and increased ingress rates in larger crack widths. Low corrosion rate (Miyazato and Hiraishi 2013) and damage (Paul and Van Zijl 2016) in embedded steel reinforcement in cracked SHCC have been reported, despite significant levels of chloride concentration at the surface of the steel bars (Paul et al. 2016). It has been postulated that crack spacing in SHCC may be of particular importance in controlling the corrosion rate, by changing the dominant electro-chemical process from macro-cell to micro-cell corrosion (Miyazato and Hiraishi 2013).

In this paper, chloride-induced corrosion in reinforced concrete (R/C), R/LWFC and R/SHCC is reported, as measured on sets of test beams, which were either pre-cracked in bending (R/C and R/SHCC), or by drying shrinkage restrained internally by the reinforcing bar (R/LWFC). Chloride profiles in cracked and uncracked regions are reported, as well as corrosion rate measurements under continuing cyclic wetting and drying with NaCl aqueous solution. The results are analysed for correlation between corrosion rate and crack spacing.

2   Experimental Program

Mix Compositions. The SHCC mix proportions by weight were 1 part water, 1 part CEM I 52.5, 1.72 parts fly-ash, 1.41 parts fine sand, and a fibre volume percentage (Vf) of 2% polyvinyl alcohol (PVA) fibre of 12 mm length and 0.04 mm diameter. Viscous modifying agent and superplasticizer are added to achieve the appropriate rheology and fibre dispersion. More details can be found in Paul (2015). The mix proportions of the concrete and LWFC are summarized in Tables 1 and 2.

For the LWFC three densities were prepared. For each density, 8 identical reference beams were prepared, of which 4 were left untreated, and the remaining 4 coated with two layers with a silane-based product with 2% active agent, subsequently referred to as surface impregnated, once the specimens were hardened. A further 4 specimens were prepared by adding a silane based water repellant agent at 2% by weight of binder in the mix, subsequently referred to as integral water repellent. This implies a total of 36 LWFC specimens. A total of 27 R/C beams were also prepared.

Table 1. R/C beams mix proportions (kg/m^3).

CEM I 52.5	Water	Fine Aggregate[a]	Coarse Aggregate[b]
467	210	425	1326

[a]Local Malmesbury river sand; [b]Local 19 mm Greywacke stone

Specimen Geometries, Casting, Curing and Pre-Cracking. *R/LWFC:* The 36 R/LWFCbeams have dimensions 460 × 100 × 100 mm (length × width × height), and a dike of dimensions 420 × 80 mm was cast into the specimens on the bottom of the casting surface of the prism, for ponding purposes during the chloride-exposure. These specimens each had a single 12 mm diameter, high tensile strength (characteristic yield

Table 2. R/LWFC mix proportions (kg/m^3).

LWFC type	Dry density	CEM I 52.5	STA[a]	Water	Foam
Reference & hydrophobic impregnated specimens	1450	1145	0	441	15
Integral hydrophobic mix	1450	1131	22.9	434	15
Reference & hydrophobic impregnated specimens	1250	995	0	383	22.6
Integral hydrophobic mix	1250	981	19.6	377	22
Reference & hydrophobic impregnated specimens	1050	844	0	325	31
Integral hydrophobic mix	1050	833	16.7	321	30

[a]STA - Silane Treatment Agent

strength of 450 MPa), ribbed steel bar embedded in the specimen, with 24 mm cover to the dike lower surface. A 6 mm diameter stainless steel bar was also embedded in each beam, for use as a counter electrode in the Coulostatic method for corrosion assessment. Further information on the Coulostatic method is given by Paul (2015). After casting and protection in the wooden moulds for 24 h, all specimens were stripped and stored in a climate controlled room at 65 ± 5% relative humidity and 23 ± 2 °C. After 28 days, the four "surface impregnated" specimens of each density were coated with the STA, and allowed to cure in the climate room with the other specimens for a further 7 days. After this, the surfaces of all beams perpendicular to the pond surface were sealed using bitumen. Cyclic ponding commenced after this, keeping the ponds filled with NaCl aqueous solution for 7 days, followed by 14 days of drying.

R/C: The 27 R/C beams of 690 × 150 × 150 mm were prepared with three different reinforcement configurations, but all with a cover of 30 mm. The first nine contained a single 10 mm diameter high strength reinforcing bar, while the second and third sets of nine contained two and three Y10 bars respectively, denoted as R1, R2 and R3. All specimens were stripped after one day, water cured at 23 ± 2 °C for 7 days, and thereafter kept in laboratory conditions at 25 ± 2 °C and relative humidity of 65 ± 5% until the testing date at the age of 28 days. The average 28-day cube compressive strength was 59.1 MPa, with a coefficient of variation (CoV) of 2.8%. Flexural four-point bending pre-cracking was performed in an Instron materials testing machine (MTM) with load-deformation responses as shown in Fig. 1a, to initiate cracks in each beam. The beams were then placed in a steel frame (Fig. 1c), and the nuts tightened to open and maintain the cracks on the upper, tensile surface at a width of 0.4 ± 1 mm. A Perspex pond of length 200 mm and the full width (150 mm) and 20 mm deep was built on the cracked, tensile face of each beam. On the sides of specimens, the cracks were sealed with silicon to prevent leakage. Cyclic ponding with NaCl solution (3 days wetting, 11 days drying) started at this point and corrosion rate measurements with a linear polarization method (GECOR 10 2015) commenced.

R/SHCC: Nine R/SHCC beams of dimensions 490 × 100 × 80 mm were prepared, each with a single 10 mm diameter high strength steel reinforcing bar. Of the nine,
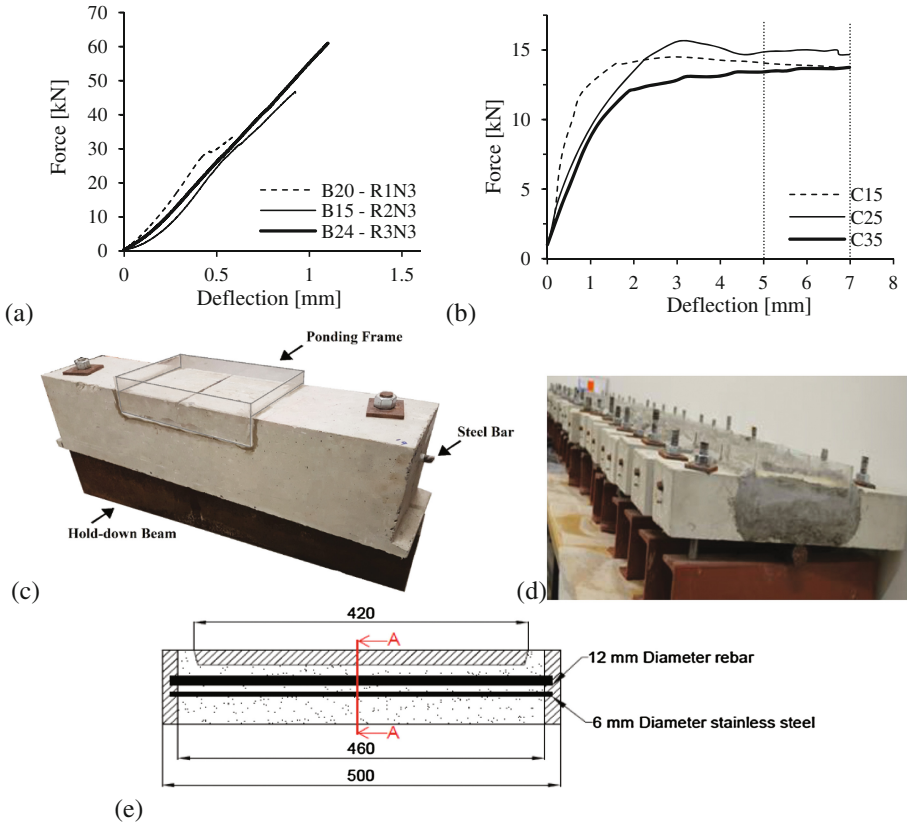
Fig. 1. Pre-cracking of (a) R/C and (b) R/SHCC beams. Setup in test frames and chloride ponding of (c) R/C, (d) R/SHCC, and (e) R/LWFC beams.

three beams had a 15 mm cover (denoted C15), three had 25 mm cover (C25) and three had 35 mm cover (C35). A 6 mm diameter, smooth stainless steel bar was placed in each beam as a counter electrode for the Coulostatic corrosion rate measurement. After casting, the beams were protected in their steel moulds, stripped after 2 days, cured in water at 23 ± 2 °C for 7 days, and subsequently in a climate room at 65 ± 5% RH and 23 ± 2 °C until the age of 14 days. They were then pre-cracked in three point bending in a Zwick Z250 MTM to form the crack patterns. Two levels of deflection were performed, i.e. 5 mm and 7 mm, and the respective specimens denoted D5 and D7. Figure 1b shows the typical pre-cracking responses. From the responses it is clear that the beams were bent to capacity, and no significant differences in crack patterns between D5 and D7 beams were observed. After pre-cracking, each beam was placed in its own steel frame (Fig. 1d), bent to the same deflection level (5, or 7 mm). A pond was subsequently built on each beam's upper, cracked face in the central part as shown in Fig. 1c. For full details, the reader is referred to Paul (2015). Similar ponding (3 days wetting, 4 days drying) started at this point.

3   Crack Width and Spacing

Figure 2 shows crack width distributions in the R/SHCC and 1450 kg/m^3 R/LWFC beams, while crack spacing distributions in R/SHCC are given in Fig. 3. Note that the cracks arose in the R/LWFC without mechanical pre-cracking, during the curing period. Tables 3 and 4 summarise the crack spacing in the R/C and R/LWFC beams respectively.

(a)   (b)
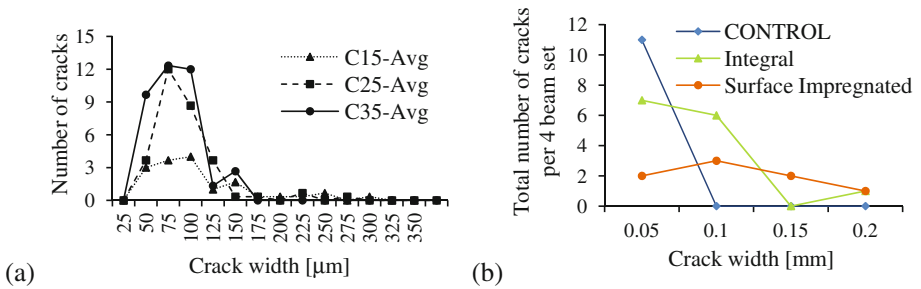
Fig. 2. Crack width distribution in (a) R/SHCC, (b) R/LWFC.

(a)
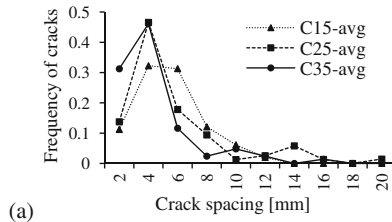
Fig. 3. Crack spacing distributions in R/SHCC.

Table 3. Crack width w_c and spacing S_c in the R/C beams at final reading (week 12).

| S_c [mm]	w_c [mm]	Nr of cracks	Nr of specimens	I_{corr} [µA/cm^2]			Cov
				Avg	Min	Max	[%]
$S_c < 85$	0.4 ± 0.1	2	6: 3R1 + 1R2 + 2R3	1.386	1.08	2.26	27.8
$85 < S_c < 100$	0.4 ± 0.1	2	8: 2R1 + 4R2 + 2R3	1.183	0.79	1.66	22.6
$S_c > 100$	0.4 ± 0.1	2	6: 1R1 + 2R2 + 3R3	1.287	1.11	1.89	24.0
Single crack	0.4 ± 0.1	1	7: 3R1 + 2R2 + 2R3	1.708	0.99	2.59	31.6

Table 4. Crack width w_c range and spacing S_c in the R/LWFC, week 12.

S_c [mm]	w_c [mm]	Nr. of cracks	Nr. of specimens	I_{corr} [µA/cm^2] Avg	Min	Max	Cov [%]
$S_c < 85$	0.05–0.15	5	5:2R1 + 2S2 + 1PB3	0.0197	0.01	0.037	55.4
$85 < S_c < 100$	0.05–0.2	5	5:4S2 + 1PB3	0.0177	0.01	0.027	41.8
$S_c > 100$	0.05–0.2	13	13:5R1 + 5S2 + 3PB3	0.0225	0.01	0.043	52.7

Note: R1 denotes Reference; S2 denotes Surface treated; PB3 denotes integral water repellent specimens

4   Chloride Profiles

Chloride profiling was performed on the R/SHCC and R/LWFC specimens in cracked and uncracked parts of the specimen exposed to cyclic ponding. X-ray fluorescence (XRF) was used to determine the Cl concentration, on powder specimens collected by drilling from the exposed tensile face of the specimens, in 3 mm intervals (SHCC) and 5 mm intervals (LWFC), into uncracked regions, as well as into cracks. Note that a 16 mm diameter drill had to be used to collect sufficient material for an XRF test, which means that the "cracked" profile includes material from the uncracked regions directly next to the cracks. Note further, that the R/SHCC profiling was done after 37 weeks of cyclic ponding, and the R/LWFC after 8 weeks of cyclic ponding. From Fig. 4a, b significantly higher chloride concentration can be seen in cracks, than in the uncracked state of both R/SHCC and R/LWFC. For the R/LWFC, it appears that the surface treated specimens perform well even in the cracks, where chloride penetration is restricted to less than 10 mm. Note that the high chloride content at positions beyond 60 mm towards the lower face of the specimen, is attributed to evaporation of water at the opposite end and deposition of chlorides in this region (Wittmann et al. 2011; Paul et al. 2016).
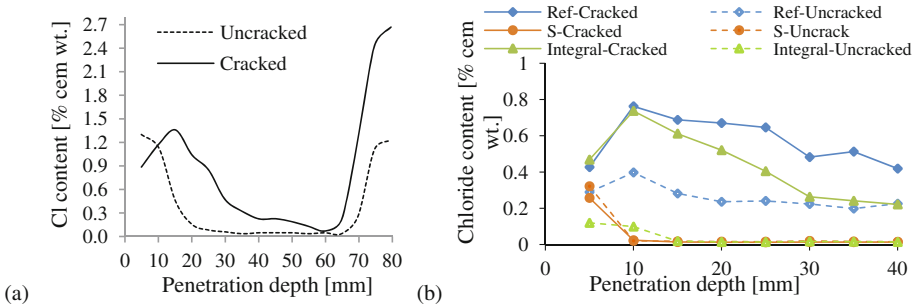

Fig. 4. Chloride penetration in uncracked and cracked (a) SHCC after 37 weeks of cyclic ponding, and (b) LWFC after 3 ponding cycles (i.e. after 9 weeks).
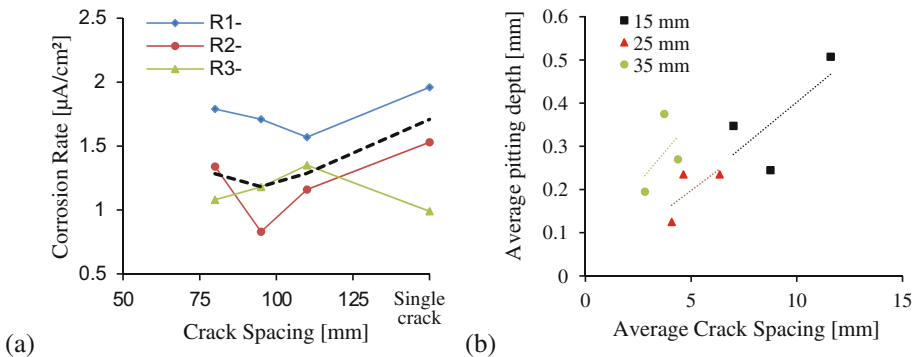
5   Corrosion Rate

The corrosion rate results are shown graphically in Fig. 5, showing an increasing trend with time. The R/C beams containing a single bar show the most significant corrosion rates. In R/LWFC, the specimens that were surface treated consistently show the lowest corrosion rates, and both treated specimens have corrosion rates well below those that are untreated. This is in agreement with the. Lower chloride contents in the treated specimens, despite the trend of wider cracks in treated specimens (Fig. 2b). Note that at the time of publication, the last readings at 11 weeks of cyclic ponding, had only been taken for the untreated specimens. Note that the readings were taken at the same stage of the ponding cycles, i.e. at the end of the drying period, just before re-filling the ponds with NaCl aqueous solution.

To investigate the role of crack spacing, Fig. 6a shows the corrosion rates at the last reading (week 12) in R/C specimens, as function of crack spacing. A more evident upward trend with crack spacing is seen in Fig. 6b, where actual steel bar corrosion damage in the R/SHCC is shown in the form of average pitting depth, measured after completion of the chloride-induced corrosion tests (37 weeks).

(a)   (b)
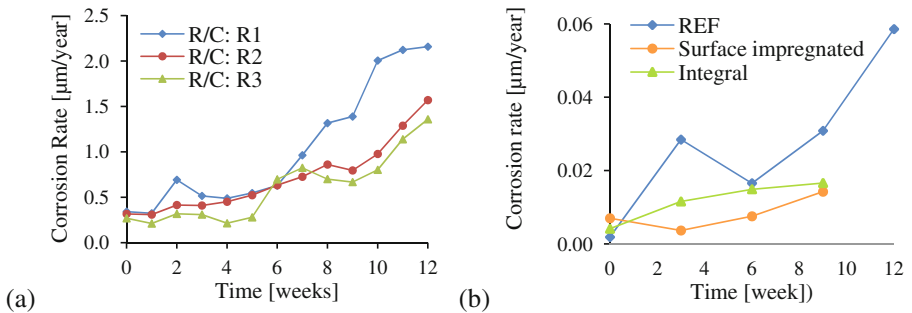
Fig. 5.   Average corrosion rate of (a) R/C and (b) R/LWFC beams.

(a)   (b)

Fig. 6.   (a) Corrosion rate in R/C as function of crack spacing after 20 weeks of ponding. (b) Pitting corrosion damage in R/SHCC specimens with 15, 25 and 35 mm cover.

6   Conclusion

From the chloride profile and corrosion rate measurement results in the respective cement-based composites, the following conclusions can be drawn:

- Chloride penetrates significantly deeper in cracked regions, than in uncracked regions, as shown by chloride profiles for R/SHCC and R/LWFC.
- Silane surface impregnation limits chloride penetration in R/LWFC, in cracked and uncracked regions. However, in integral water repellent LWFC, which contains silane in the mix, cracks allow ingress of significant levels of chloride to penetrate deep into R/LWFC.
- Chloride-induced corrosion appears to be higher for beams with larger crack spacing. This trend is most evident in R/SHCC.

The tests on R/C and R/LWFC are ongoing, and will end by mass loss measurements of the steel reinforcement bars to verify actual corrosion damage.

References

Boshoff, W.P., Altmann, F., Adendorff, C.J., Mechtcherine, V.: A new approach for modelling the ingress of deleterious materials in cracked strain hardening cement-based composites. Mater. Struct. **49**, 2285–2295 (2016)

Djerbi, A., Bonnet, S., Khelidj, A., Baroghel-Bouny, V.: Influence of traversing crack on chloride diffusion into concrete. Cem. Concr. Res. **38**, 877–883 (2008)

GECOR 10 (2015). http://www.isdcorr.com/www.isdcorr.com/GECOR_10_files/GECOR%2010_2015_ENG.pdf. Accessed 15 Jan 2017

Miyazato, S., Hiraishi, Y.: Durability against steel corrosion of HPFRCC with bending cracks. J. Adv. Concr. Technol. **11**, 135–143 (2013)

Paul, S.C.: The role of cracks and chlorides in corrosion of reinforced strain hardening cement-based composite (R/SHCC). Ph.D. Dissertation, Stellenbosch University (2015)

Paul, S.C., Van Zijl, G.P.A.G.: Chloride-induced corrosion modelling of cracked reinforced SHCC. Arch. Civ. Mech. Eng. **16**(4), 734–742 (2016)

Paul, S.C., Van Zijl, G.P.A.G., Babafemi, J., Ming Jen, T.A.N.: Chloride ingress in cracked and uncracked specimens made from strain hardening cement-based composite (SHCC). Constr. Build. Mater. **114**(2016), 232–240 (2016)

Wittmann, F.H., Wang, P., Zhang, P., Zhao, T., Beltzung, F.: Capillary absorption and chloride penetration in neat and water repellent SHCC under imposed strain. In: Proceedings of the 2nd International RILEM Conference on Strain Hardening Cementitious Composites, Brazil, pp. 165–172 (2011)